# A NEW FIELD ORIENTED CONTROL WITH SYNERGETIC CONTROL FOR AN URBAN ELECTRIC VEHICLE

Idris Azizi<sup>12\*</sup> – Brahim Dahraoui<sup>1</sup> – Ismail Haddi<sup>1</sup> –Farid Belouahchi<sup>2</sup>

<sup>1</sup>Department of Electrotechnic, Faculty of Technology Sciences, University of Mentouri Brothers Constantine -1-, Constantine, Algeria

<sup>2</sup>Laboratory of Automatic (LAS), Technology Faculty, University of Setif -1-, Setif, Algeria

#### **ARTICLE INFO**

## Article history:

Received: 28.12.2024.

Received in revised form: 07.12.2024.

Accepted: 13.12.2024

#### Keywords:

Synergetic control
Bidirectional converter
Electric vehicle
Field orientation control
Vehicle dynamics

DOI: https://doi.org/10.30765/er.2658

#### Abstract:

This paper suggests a new field-oriented control strategy based on synergetic control for an urban electric vehicle propelled by a Permanent Magnet Synchronous Machine (PMSM). The overall study system is explained, with a synergetic approach, no linearization or simplification of the model is required. The method of controllers' synthesis is analytical and it depends on non-linear models of the PMSM, also, to design the proposed synergetic controllers, three-manifolds of stator current and the speed of the propel PMSM are selected. A comparison study between the proposed strategy and the conventional one based on PI controllers using a dynamic model of a lightweight vehicle is established. The simulation results show the proposed control's superiority, robustness, and effectiveness in static and dynamic performances; this has a direct impact on the vehicle's comfort and energy consumption.

### 1 Introduction

The continued expansion of the global economy, population growth, and improvements in people's quality of life all contribute to increased energy usage and consumption. It also harms the environment and accelerates global warming [1], [2]. Exhaust emissions from vehicles are the main cause of greenhouse gas impacts, with the main emissions being carbon monoxide (CO) and carbon dioxide (CO2). These pollutants contribute significantly to the development of lung cancer and other serious respiratory diseases. The transportation sector consumes around 50% of world oil supplies and contributes to 25% of global CO2 emissions [2], [3]. As a result, research institutes and companies have long defended electric vehicles (EVs) as a viable substitute for conventional vehicles, particularly in urban areas [4]. The EV is only propelled by one or more electrical motors and is entirely powered by electrical energy from the power storage unit. The primary drawback of EVs is the problem of energy storage. Numerous studies have been conducted to improve efficiency, lower the cost of manufacture, and prolong the EVs' driving range. Therefore, as power electronics and Energy Storage Systems (ESSs) are constantly improving, EVs would be capable of competing with conventional ones [5], [6]. One effective way to increase an electric vehicle's range and reduce the size of its ESS is to convert kinetic energy into electrical energy throughout braking and provide it to an ESS [7]. References [8] and [9] highlighted the fact that with regenerative braking, the EV range may rise from 8% to 33%. One of the most preferred choices for Electric and Hybrid Electric vehicle applications is the PMSM, this is because of its fast torque response, superior power density, high efficiency, and the possibility of a noiseless function as compared to an asynchronous motor [10], [11]. Since the EV is a multi-subsystem complex physical system, modeling each subsystem is a difficult process that necessitates in-depth vehicle kinematic and dynamic studies. Moreover, controlling the EV while taking into account several of factors that affect its behavior, such as nonlinearities, unmeasured disturbances, and system parameter uncertainty, necessitates the use of strong, robust, and insensitive control strategies. As a result, several studies have shown position and speed control

E-mail address: dris.azizi@umc.edu.dz

<sup>\*</sup> Corresponding author

using various driving and control strategies [12]. By separately controlling the torque and flux, similar to independently excited DC motors, the technique of Indirect Field Oriented Control (IFOC) may be used for controlling an extensive range of AC motors, from synchronous to asynchronous [13]. This method is based on linear controllers, such as the Proportional-Integral-Differential (PID) and Proportional-Integral (PI) controllers. The principal advantages of these controllers are their ease of synthesis and simplicity of implementation. Nevertheless, they are insufficiently robust against an unmeasured disturbance and the controlled system's parameter uncertainty [12]. To resolve these problems, where little research has been done, including in [14], [15], [16], the application of a non-linear technique is crucial, including fuzzy logic, that is viewed as among the most effective artificial intelligence methods used to control nonlinear systems, as well as sliding mode control (SMC), that ensures stable system and good robustness to parametric variations and external disturbance [17], [18], [19]. Authors in papers [20], [21], [22] demonstrated that using PI control with gains adaptation based on adaptive fuzzy and adaptive neuro-fuzzy inference system can overcome the parameters variations. Furthermore, PI-backstepping control is robust against external torque disturbances and parameter variations. The major drawback of SMC is the phenomenon of chattering, which degrades system performance by leading to low control accuracy, excessive wear of mechanical parts and significant heat loss in the circuits. The phenomenon of chattering is a major obstacle to the use of SMC [23], [24].

The synergistic approach is proposed in [25]. This method is a viable choice for controlling nonlinear uncertain systems in disturbed situations. That is why various researches have been undertaken in this area [26], [27], [28], [29], [30]. The synergistic control (SC) technique is similar to the SMC approach in that it employs a shared methodology, mainly the imposition of a dynamic predetermined by the designer, but without the disadvantages of the SMC technique. The synergetic control is appropriate for digital control implementation and practice, as it needs a relatively low bandwidth for the controller, second it works at a constant switching frequency and lacks the chattering problems of SMC, which reduces power filtering problems [31]. In addition, it can decrease the size of a modeled system and guarantee the power system stability in general [12]. These above advantages highlight the importance of using this type of controller for PMSMs in EV applications. In this paper, we propose a new IFOC scheme based on a SC approach for an EV propelled by PMSM drive which the goal is to achieve high performances of the control applied. We test the proposed approach performances for a known displacement of a lightweight EV under different operating conditions. The simulation results show the superiority and effectiveness of the suggested approach compared with a scheme based on classical control using PI controllers.

## 2 System description and modeling

The EV's powertrain consists of an ESS, a bidirectional DC-DC converter, and a PMSM drive. Figure 1 depicts the system structure under study.

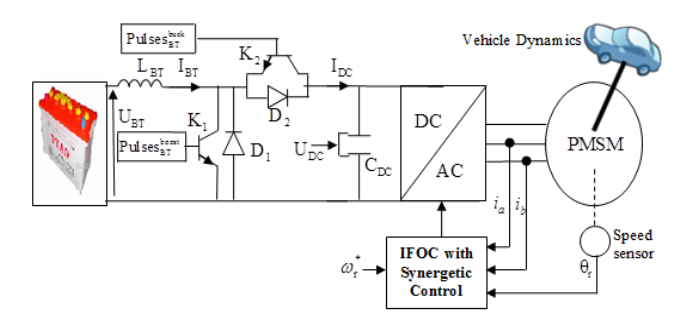


Figure 1. The block diagram of the proposed system.

The PMSM is controlled via the IFOC. The applied load torque which is the vehicle dynamics allows the definition of two operation modes: when the applied torque is positive, this is the motor mode, the DC-DC converter behaves as a boost converter at which  $K_1$  and  $D_2$  are active, energy flows to the DC-Link raising the voltage level that supplies the motor, (for example, the vehicle encounters a high hill); and when the applied torque is negative, this is regenerative braking mode, the DC-DC converter behaves as a buck converter at witch  $K_2$  and  $D_1$  are active, energy flows from the DC-Link to the battery (for example the vehicle encounters a downhill). The DC link current, IDC, may be positive or negative while the DC bus voltage is always positive

[32], [33], [34]. In a cascade configuration, the DC-DC converter is controlled by two loops: the inner loop employs a hysteresis controller to regulate the current, whereas the outer loop employs a PI controller to regulate the DC bus voltage, as shown in Figure 2.

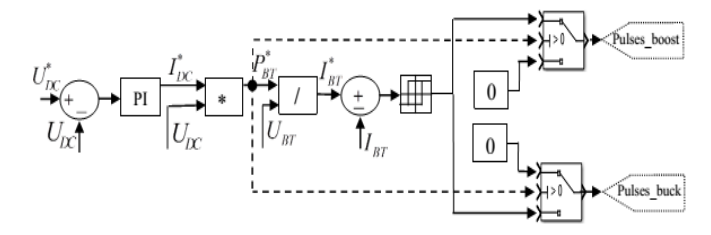


Figure 2. Control of DC-DC converter with cascade configuration.

In the DC-link, the power flow capacitor is represented by this equation:

$$P_{DC} = \frac{dE_{DC}}{dt} = P_{bat} - P_{Load} = C_{DC} \frac{dU_{DC}}{dt} U_{DC}$$
 (1)

 $P_{DC}(W)$  is the resulted DC-link power,  $E_{DC}$  (J) is the energy stocked in the DC-bus capacitor,  $P_{bat}$  (W) is the power transferred between the batteries and the DC-link,  $P_{Load}(W)$  is the requested power from the load;  $C_{DC}(F)$  is the capacitor, and  $U_{DC}(V)$  the DC bus voltage.

## 2.1 The PMSM Drive

A three-phase voltage source inverter with six IGBT and six anti-parallel diodes mounted in a bridge configuration supplies the PMSM [35].

# 2.1.1 The PMSM model

There are two modes of operation for the PMSM block: generating and motoring. The induced electromagnetic force is assumed to be sinusoidal. The equations below, which are represented in the rotor reference frame (dq frame), can be utilized to describe the electrical and mechanical systems of the PMSM model [36], [37], [38].

$$\begin{cases} d/dt^{i_{sd}} = \frac{1}{L_d} v_{sd} - \frac{R_s}{L_d} i_{sd} + \frac{L_q}{L_d} p \omega_r i_{sq} \\ d/dt^{i_{sq}} = \frac{1}{L_d} v_{sq} - \frac{R_s}{L_q} i_{sq} - \frac{L_d}{L_q} p \omega_r i_{sd} - \frac{\lambda p \omega_r}{L_{sq}} \\ T_e = 1.5 p \left[ \lambda i_{sq} + (L_d - L_q) i_{sd} i_{sq} \right] \end{cases}$$
(2)

$$\begin{cases}
\frac{d}{dt}\omega_r = \left(\frac{1}{J}T_e - F\omega_r - T_L\right) \\
\frac{d\theta_r}{dt} = \omega_r
\end{cases}$$
(3)

 $i_{sd},i_{sq}$  (A): d-q axis currents of the stator,  $v_{sd}$ ,  $v_{sq}$  (V): d-q axis voltages of stator,  $L_d$ ,  $L_q$ : d-q axis inductance of stator,  $R_S$ : stator windings resistance, p: pole pairs number,  $\omega_r$  (rad/s): the mechanical speed,  $T_e$  (N.m): electromagnetic torque and  $\lambda$  (Wb): the rotor magnet flux, F (N.m.s): coefficient of Viscous Friction, J (kg.m2): inertia of Rotor and  $\theta_r$  (rad): the mechanical rotor angle.

For this work, a surface permanent magnet synchronous machine is selected, where  $L_d = L_q = L_s$ , features no saliency, a uniform air gap, and the magnets are placed on the rotor's surface [36].

, and the second second

### 2.1.2 Indirect Field oriented control method

Figure 3 depicts the IFOC's block diagram of the PMSM drive, where the reference current  $i_{sq}^*$  is obtained from an outer speed control loop, and  $i_{sd}^*$  is obtained after using the block of flux weakening as outlined in [9]. The errors of stator currents are regulated by PI controllers that make the stator reference voltages  $v_{sd}^*$  and  $v_{sq}^*$ . Then, the obtained voltages are transformed to the abc phase variables and supplied to the inverter using the PWM technique [13]. For the strategy of IFOC with SC, as illustrated in Figure 3, synergetic controllers replace the conventional PI controllers for the PMSM's speed and currents, and the voltage decoupling block is removed.

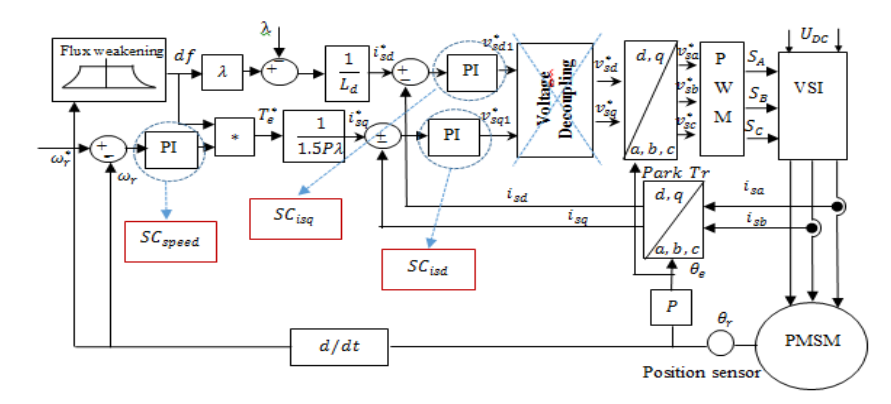


Figure 3. Diagram of the IFOC principle with classical and synergetic control.

## 3 Synthesis of Synergetic Approach

In general, nonlinear systems are represented dynamically as follows [39], [40], [41].

$$\dot{X} = f\left(X, u, t\right) \tag{4}$$

x: The system state vector, u: the control vector and t: represents time.

To design a synergetic control, the first step is to determine of a macro-variable that is a function of the system's state variables.

$$\psi = \psi(X, t) \tag{5}$$

 $\Psi$  represents the macro-variable and  $\psi(X, t)$  a function selected by the user. To examine the various constraints applied on the system, we modify the macro-variable based on the constraint to examine, the system is compelled to function on the manifold using the control  $\Psi = 0$ .

Step two involves determining the required dynamic development of the macro-variable to the manifold  $\Psi = 0$  using the following general equation [39], [40].

$$T\dot{\psi} + \psi = 0 \tag{6}$$

T represents the control parameter that specifies the speed of convergence to the manifold defined by the macrovariable. Equation (6)'s solution yields the following function:

$$\psi(t) = \psi_0 \rho^{-\frac{t}{\tau}} \tag{7}$$

Considering the differentiation chain, which is presented by [40], [42], [43]:

$$\frac{d\psi(X,t)}{dt} = \frac{d\psi(X,t)}{dX}\frac{dX}{dt} \tag{8}$$

Substituting equations (5) and (6) into (8), we obtain:

$$\frac{d\psi(X,t)}{dt}f(X,u,t)+\psi(X,t)=0$$
(9)

The control law that results from solving equation (9) for u is as follows[36], [37], [38]:

$$u = g(X, \psi(X, t), T, t) \tag{10}$$

It is evident from equation (10), that the control is related to the macro-variable and the control parameter T in addition to the system's variable state. It indicates that the designer's selection of appropriate macro-variables and parameters of specific control T determines the controller's features. In the above-mentioned synthesis of a synergic controller, it is noted that this controller works with a non-linear system, therefore no model simplification or linearization is required, as is usually with conventional control systems [44].

# 4 Synergetic Controllers Design for PMSM

## 4.1 Speed control

To design a synergetic controller for the rotation speed of the PMSM, we analyse the equation of state that describes the dynamics of the motor shaft:

$$\frac{d}{dt}\omega_r = \dot{\omega}_r = \frac{1}{J}(T_e - F\omega_r - T_L) \tag{11}$$

We choose the speed error as the macro-variable:

$$\Psi(\omega_r) = e(\omega_r) = \omega_r^* - \omega_r \tag{12}$$

The derivative of the macro-variable function is:

$$\dot{\Psi}(\omega_r) = -\omega_r \tag{13}$$

Based on (6), (11), (12), and (13), the control law  $T_e^*$  is then expressed as follows:

$$T_e^* = \frac{J}{T_{\omega_r}} \left[ (\omega_r^* - \omega_r) + \frac{T_{\omega_r}}{J} T_L + \frac{T_{\omega_r}}{J} F \omega_r \right]$$
 (14)

## 4.2 Direct current control

To design the synergetic controller of the direct current  $i_{sd}$ , we consider the system of equation (15):

$$\frac{d}{dt}i_{sd} = \frac{v_{sd}}{L_d} - \frac{R_s i_{sd}}{L_d} + \omega_r L_q \frac{i_{sq}}{L_d}$$
(15)

We choose the direct current error as the macro-variable:

$$\psi(i_{sd}) = e(i_{sd}) = i_{sd}^* - i_{sd}$$
 (16)

The macro-variable function's derivative is:

$$\Psi(i_{sd}) = -i_{sd}^{\mathcal{K}} \tag{17}$$

Considering (6), (15), (16) and (17), the control law  $v_{sd}$  is then formulated as follows:

$$v_{sd} = \frac{L_d}{T_{i_{sd}}} \begin{pmatrix} (i_{sd}^* - i_{sd}) + \frac{T_{i_{sd}} R_s i_{sd}}{L_d} \\ -T_{i_{sd}} \omega_r L_q \frac{i_{sq}}{L_q} \end{pmatrix}$$
(18)

## 4.3 Quadrature current control

To design the synergetic controller of the quadrature current  $i_{sq}$ , we consider the system of equation (19):

$$\frac{d}{dt}i_{sq} = \frac{v_{sq}}{L_q} - \frac{R_s i_{sq}}{L_q} - \omega_r L_d \frac{i_{sd}}{L_q} - \frac{\omega_r}{L_q} \varphi_f$$
(19)

We choose the quadrature current error as the macro-variable:

$$\psi(i_{sq}) = e(i_{sq}) = i_{sq}^* - i_{sq}$$
 (20)

The macro-variable function's derivative is:

$$\Psi(i_{sa}) = -i_{sa}^{\&} \tag{21}$$

Considering (6), (19), (20) and (21), the control law  $v_{sq}$  is then written:

$$v_{sq} = \frac{L_q}{T_{i_{sq}}} \begin{pmatrix} (i_{sq}^* - i_{sq}) + \frac{T_{i_{sq}} R_s i_{sq}}{L_q} \\ + T_{i_{sq}} \omega_r L_q \frac{i_{sd}}{L_q} + \frac{T_{i_{sq}} \omega_r}{L_q} \varphi_f \end{pmatrix}$$
(22)

 $T_{\omega_{r}}$ ,  $T_{i_{sd}}$  and  $T_{i_{sq}}$ : are chosen so as to have satisfactory static and dynamic performances.

## 5 Vehicle dynamics

As shown in Figure 4, consider a vehicle with mass M (kg) moving at a speed of v (m/s) up a slope of angle  $\alpha$  (rad) [45], [46], [47], [48]:

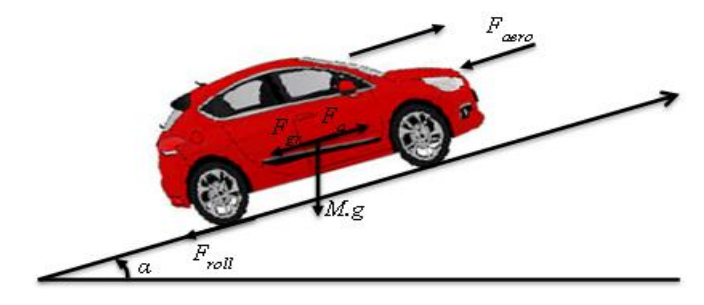


Figure 4. Forces exerted on a vehicle traversing up a high hill.

Considering the vehicle on an inclined track, the required tractive effort is:

$$F_{te} = F_a + F_{or} + F_{roll} + F_{aero} (23)$$

The first force is the acceleration force, which has a positive sign in the acceleration phase and a negative sign in the deceleration phase. The second resistance is applied as the vehicle climbs a hill, which is determined by the slope of the road; it is called gradient resistance. The third resistance force is rolling resistance Froll, and it is caused by the flattening of the tire on the roadway contact surface. The fourth is the aerodynamic drag  $F_{\text{aero}}$ .

$$\begin{cases} F_{a} = \pm M_{e} \frac{dv}{dt} \\ F_{gr} = \pm M.g.\sin\alpha \\ F_{roll} = M.g.\mu \\ F_{aero} = 0.5.C_{d}.\rho.A_{f}.(v \pm v_{wind})^{2} \end{cases}$$
(24)

Me is the equivalent mass, g: Gravity of Earth,  $\mu$ : coefficient of tire rolling resistance, Cd: coefficient of aerodynamic drag, $\rho$ : density of Air,  $A_f$ : frontal area of Vehicle, and  $v_{wind}$ : wind speed (m/s).

$$M_e = \delta M \tag{25}$$

 $\delta$  represents rotational inertia factor or the mass factor:

$$\delta = 1 + 0.04 + 0.0025i^2 \tag{26}$$

Where i is the gear ratio.

The electromagnetic torque and the vehicle global inertia moment in the motor referential are respectively given by:

$$T_e = \frac{T_{te}}{i} = \frac{r}{i} F_{te} \tag{27}$$

$$J_T = \frac{M_e r^2}{i^2} \tag{28}$$

 $T_{te}$  (N.m) represents motor torque on the wheels, r is the tire radius.

The equation that describes the electric motor dynamic behavior, in the motor referential, is presented as follows:

$$T_e - T_L = J_T \frac{d\omega_r}{dt} \tag{29}$$

T<sub>L</sub> (N.m) is the load torque applied on the motor shaft.

## 6 Simulation Results

Using Matlab/Simulink software, a simulation model has been built to evaluate and compare the control of the suggested strategy with one based on PI controllers. Table 1 displays the parameters of the simulation.

Table 1. Parameters of Simulation.

	Battery converter	Load converter
Converter topology	bidirectional converter	Sinusoidal Pulse Width Modulation inverter Switching frequency:20KHz
Technic of Control	cascade control (hysteresis controllers +PI).	IFOC
Sample times: System discrete:Ts=5e-6s	Tc_DC_bus_=10*Ts Tc_Battery_cont- roller=10*Ts	IFOC: T <sub>IFOC</sub> =10*Ts Speed controller: Tc_speed=7*10*Ts
Control Parameters	DC bus Voltage controller:(kp,ki)= ( 2.12,450) Current_Battery: Δi=±1	Controller of Speed:(kp,ki)=( 227.65, 16100) Direct current controller:(kp,ki)=( 1.79, 2668.5) Quadrature current controller:(kp,ki)=( 1.79, 2668.5) Synergetic controllers: $(T_{\omega_{\Gamma}}, T_{i_{sd}}, T_{i_{sg}})$ =(0.000625,0.00005,0.0000925)

The EV was tested with an acceleration/deceleration of  $\pm 2.135$  m/s<sup>2</sup> at a 30 km/h reference speed. At 15 and 25 seconds, the vehicle faces a high hill with slopes of 10% and 13.33%, respectively; then at 30 seconds, the EV encounters a downhill with a slope of -5%; and at 40 seconds, the EV continues moving with no slope until stopping. The battery SOC (state of charge) was assumed to be 80%. Tables 2 and 3 describe the parameters of the EV and motor, respectively.

Table 2. Vehicle Body Parameters.

Parameter	Value	Parameter	Value
vehicle Masse M (kg)	1150	frontal area of Vehicle A <sub>f</sub> (m <sup>2</sup> )	2.5
coefficient of aerodynamic drag C <sub>d</sub>	0.32	radius of Wheel r(m)	0.33
coefficient of tire rolling resistance µ	0.015	Gravity of Earth g (m/s <sup>2</sup> )	9.81
gear ratio i	10	density of Air $\rho(kg/m^3)$	1.28

Table 3. PMSM Parameters.

Parameter	Value	Parameter	Value
Nominal power (KW)	35	Inertia of rotor J (kg.m <sup>2</sup> )	0.05
Nominal speed (tr/min)	3000	DC voltage (Volt)	560
Nominal torque (N.m)	111	Pole pairs Number p	4
The stator windings Resistance $R_S(\Omega)$	0.05	$\begin{array}{c} \text{Inductance of Stator $L_d$, $L_q$} \\ \text{(mH)} \end{array}$	0.635

Figure 5 below shows the EV's linear speed, electromagnetic torque, and currents for this test using synergetic and traditional controls. The SC has a high performance and strong robustness compared with PI controls. While the synergetic speed controller showed roughly no overshoot (0.001 km/h), the PI controller showed a measurable overshoot of 0.036 km/h. Additionally, we observe that the synergetic controller performs well in terms of precision and load torque rejection, with a faster torque response time and very small tracking static error of speed (0.00025 km/h) compared to 0.00072 km/h for the PI controller case. Furthermore, the proposed control has fewer ripples in the electromagnetic torque (17 N.m) than the conventional control (30 N.m).

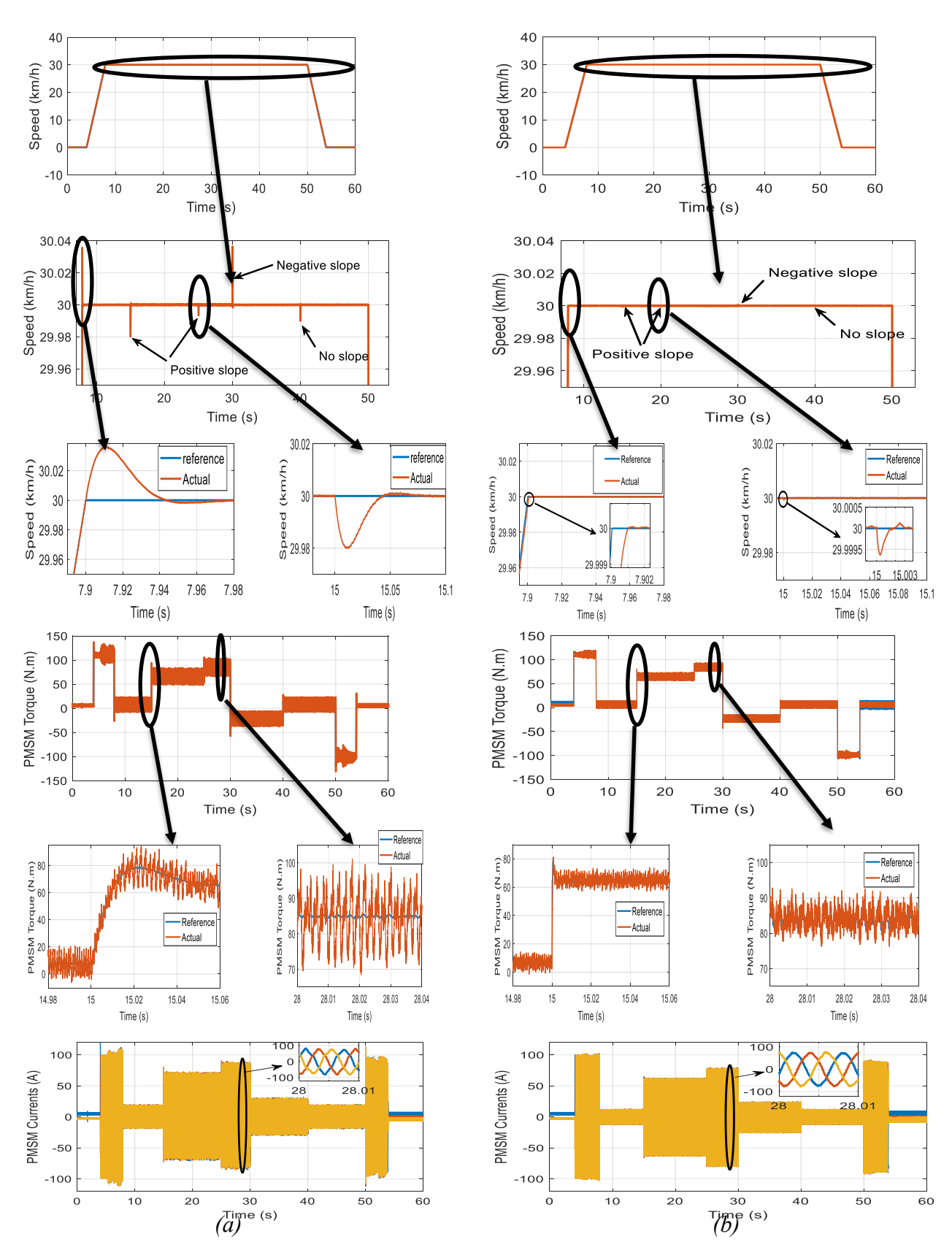


Figure 5. Simulations results for the movement of an EV using IFOC with classical control (a) and synergetic control (b).

The comparison of the Total Harmonic Distortion (THD) of stator currents between the two strategies is illustrated in Figure 6. With PI controllers, the stator current THD is approximately 9.21%. In contrast, the proposed control scheme significantly reduces the stator current THD to about 3.83%, showing minimal distortion in the stator current.

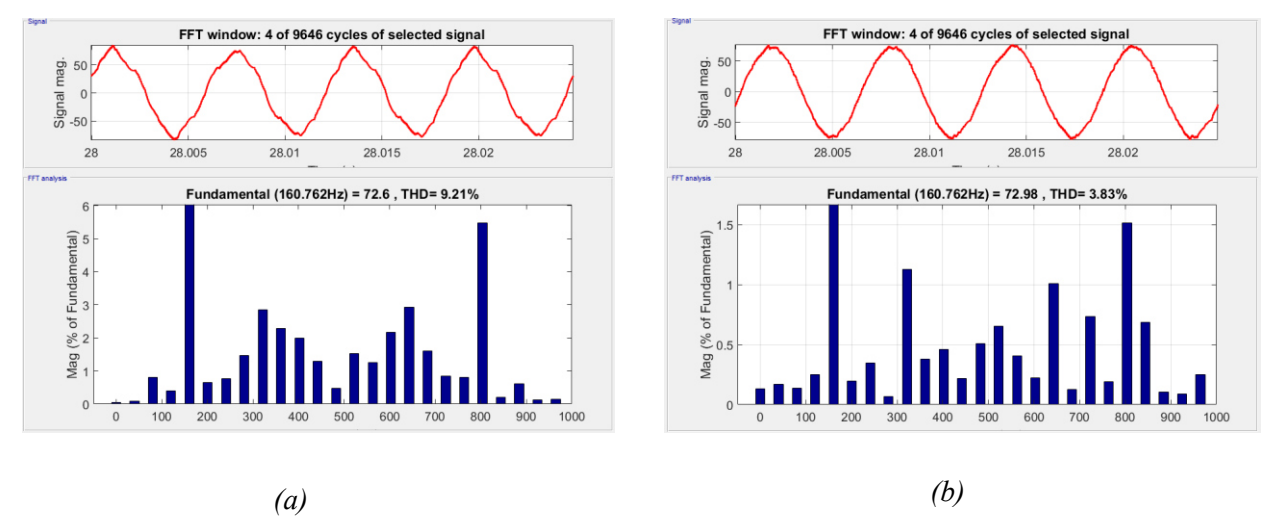


Figure 6. a\_phase stator current and its Harmonics spectrum with classical control (a) and synergetic control (b).

Table 4 summarizes the comparative analyses between the proposed synergetic controllers and PI controllers

	Speed Overshoot km/h	Speed error (km/h)	Torque ripple (N.m)	THD stator current
PI Controllers	0.036	0.00072	30	9.21%
Synergetic Controllers	0.001	0.00025	17	3.83%

*Table 4. Comparative analysis using synergetic and PI controllers.* 

A simulation is developed to test the ESS and consumed energy using the ECE-15 urban drive cycle. In Figure 7, the speed, source energy, and SOC are presented. The integration of the power output at the terminals of the battery across the whole cycle gives energy consumption.

It's clear that with synergetic control, the EV tracks almost perfectly the speed reference, with very minor fluctuations; these improvements directly affect the EV's comfort. The results show that the energy consumed for moving the EV with conventional control is 413452 J. Meanwhile a 412356 J is necessary when using synergetic control. These results confirm the effectiveness of the suggested control.

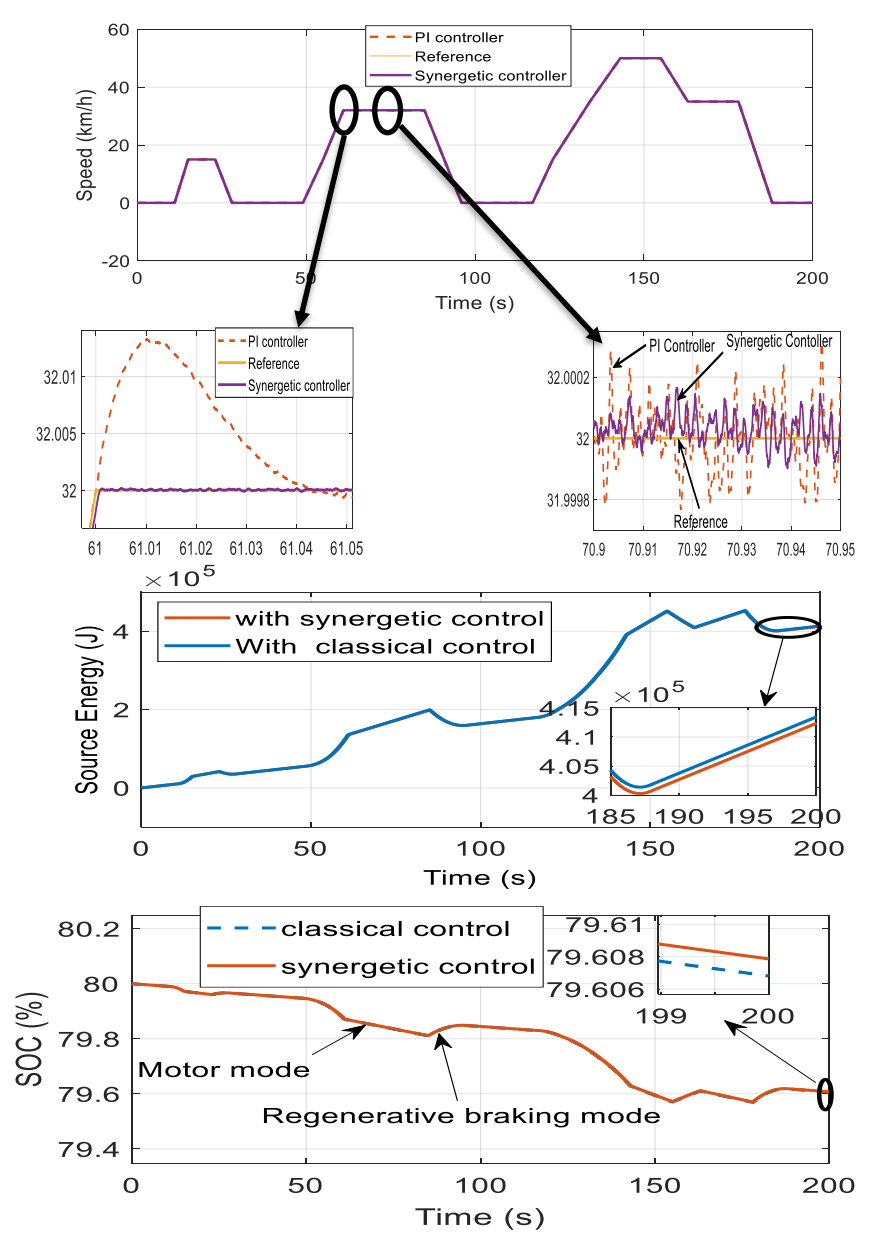


Figure 7. Simulation Results of an urban drive cycle ECE-15 with classical and synergetic controls.

## 7 Conclusion

In this work, we presented a new technic of IFOC with synergetic control for an urban EV propelled by a PMSM where the system functions in motor and regenerative braking modes. The simulation results show that the proposed strategy based on SC permits better performance than the classic strategy based on PI controllers in terms of accuracy, time response, THD stator current, electromagnetic torque ripples, load torque rejection, and robustness. The static speed error is less than approximately two-thirds compared to the classical control, and the THD stator current does not exceed 5%. Using the cycle urban ECE15, it is demonstrated that synergetic control is successful, as it can reduce energy consumption by 1096 J for only 200 s, which increases the vehicle's autonomy.

Our future studies include:

- Testing the robustness of the proposed strategy by the variation of parameters system like the inertia moment and testing the speed tracking in case of slow and fast dynamic speed command.
- Comparing this strategy with other strategies such as sliding mode control, predictive control, etc.

. 1221, D. Danidoui, I. 11aai, I. Beloudien. 11 new field of tened control with synergetic control ...

### References

[1] D. Söffker, "Towards Optimal Power Management of Hybrid Electric Vehicles in Real-Time: A Review on Methods, Challenges, and State-Of-The-Art Solutions", Energies, vol. 11, Feb. 2018, doi: 10.3390/en11030476.

- [2] M. Abdelsattar Mohamed Saeed, M. M. Aly, and S. Abu-Elwfa, "A Review on Hybrid Electrical Vehicles: Architectures, Classification and Energy Management", SVU-Int. J. Eng. Sci. Appl., vol. 5, no. 2, pp. 93–99, Dec. 2024, doi: 10.21608/svusrc.2024.263668.1177.
- [3] A. Zobaa and B. Bose, "Renewable Energy, Global Warming Problem and Impact of Power Electronics", Renew. Energy Power Qual. J., pp. 1–10, May 2011, doi: 10.24084/repqj09.003.
- [4] A. Nouh, "Contribution au développement d'un simulateur pour les véhicules électriques routiers", Besançon, 2008. See http://www.theses.fr/2008BESA2013
- [5] A. Khaligh and Z. Li, "Battery, Ultracapacitor, Fuel Cell, and Hybrid Energy Storage Systems for Electric, Hybrid Electric, Fuel Cell, and Plug-In Hybrid Electric Vehicles: State of the Art", IEEE Trans. Veh. Technol., vol. 59, no. 6, pp. 2806–2814, Jul. 2010, doi: 10.1109/TVT.2010.2047877.
- [6] J. P. Trovão, P. G. Pereirinha, H. M. Jorge, and C. H. Antunes, "A multi-level energy management system for multi-source electric vehicles An integrated rule-based meta-heuristic approach", Appl. Energy, vol. 105, no. C, pp. 304–318, 2013.
- [7] J. Armenta, C. Núñez, N. Visairo, and I. Lázaro, "An advanced energy management system for controlling the ultracapacitor discharge and improving the electric vehicle range", J. Power Sources, vol. 284, pp. 452–458, Jun. 2015, doi: 10.1016/j.jpowsour.2015.03.056.
- [8] M. K. Yoong et al., "Studies of regenerative braking in electric vehicle", in 2010 IEEE Conference on Sustainable Utilization and Development in Engineering and Technology, Nov. 2010, pp. 40–45. doi: 10.1109/STUDENT.2010.5686984.
- [9] I. Azizi and H. Radjeai, "Motor and Regenerative Braking Operations for an Electric Vehicle using Field Oriented Control", in 2022 19th International Multi-Conference on Systems, Signals & Devices (SSD), May 2022, pp. 2145–2150. doi: 10.1109/SSD54932.2022.9955671.
- [10] T. D. Batzel and K. Y. Lee, "Electric propulsion with sensorless permanent magnet synchronous motor: implementation and performance", IEEE Trans. Energy Convers., vol. 20, no. 3, pp. 575–583, Sep. 2005, doi: 10.1109/TEC.2005.852956.
- [11] A. Choudhury, P. Pillay, and S. S. Williamson, "DC-Link Voltage Balancing for a Three-Level Electric Vehicle Traction Inverter Using an Innovative Switching Sequence Control Scheme", IEEE J. Emerg. Sel. Top. Power Electron., vol. 2, no. 2, pp. 296–307, Jun. 2014, doi: 10.1109/JESTPE.2013.2296973.
- [12] M. K. B. Boumegouas and K. Kouzi, "A New Synergetic Scheme Control of Electric Vehicle Propelled by Six-phase Permanent Magnet Synchronous Motor", Adv. Electr. Electron. Eng., vol. 20, no. 1, Art. no. 1, Mar. 2022, doi: 10.15598/aeee.v20i1.4221.
- [13] F. Yusivar, N. Hidayat, R. Gunawan, and A. Halim, "Implementation of field oriented control for permanent magnet synchronous motor", in 2014 International Conference on Electrical Engineering and Computer Science (ICEECS), Nov. 2014, pp. 359–362. doi: 10.1109/ICEECS.2014.7045278.
- [14] G. Boukhalfa, S. Belkacem, A. Chikhi, and S. Benaggoune, "Direct torque control of dual star induction motor using a fuzzy-PSO hybrid approach", Appl. Comput. Inform., vol. 18, no. 1/2, pp. 74–89, Jan. 2020, doi: 10.1016/j.aci.2018.09.001.
- [15] Y. Yue and L. Yan, "A Novel Sensorless Fuzzy Sliding-Mode Control of Induction Motor", Int. J. Control Autom., vol. 8, pp. 1–10, Sep. 2015, doi: 10.14257/ijca.2015.8.9.01.
- [16] A. Khedher and M. Faouzi Mimouni, "Sensorless-adaptive DTC of double star induction motor", Energy Convers. Manag., vol. 51, no. 12, pp. 2878–2892, Dec. 2010, doi: 10.1016/j.enconman.2010.06.028.
- [17] H. Amimeur, D. Aouzellag, R. Abdessemed, and K. Ghedamsi, "Sliding mode control of a dual-stator induction generator for wind energy conversion systems", Int. J. Electr. Power Energy Syst., vol. 42, no. 1, pp. 60–70, Nov. 2012, doi: 10.1016/j.ijepes.2012.03.024.
- [18] Z. Yan, C. Jin, and V. Utkin, "Sensorless sliding-mode control of induction motors", IEEE Trans. Ind. Electron., vol. 47, no. 6, pp. 1286–1297, Dec. 2000, doi: 10.1109/41.887957.
- [19] A. Kolesnikov et al., "A synergetic approach to the modeling of power electronic systems", in COMPEL 2000. 7th Workshop on Computers in Power Electronics. Proceedings (Cat. No.00TH8535),

\_\_\_\_\_

- Jul. 2000, pp. 259–262. doi: 10.1109/CIPE.2000.904726.
- [20] C. Regaya, F. Fethi, A. Zaafouri, and A. Chaari, "Adaptive proportional-integral fuzzy logic controller of electric motor drive", Eng. Rev., vol. 41, Jan. 2021, doi: 10.30765/er.1446.
- [21] C. B. Regaya, F. Farhani, H. Hamdi, A. Zaafouri, and A. Chaari, "Robust ANFIS Vector Control of Induction Motor Drive for High-Performance Speed Control Supplied by a Photovoltaic Generator", WSEAS Trans. Syst. Control, vol. 15, pp. 356–365, 2020, doi: 10.37394/23203.2020.15.37.
- [22] F. Farhani, C. Ben Regaya, A. Zaafouri, and A. Chaari, "Real time PI-backstepping induction machine drive with efficiency optimization", ISA Trans., vol. 70, pp. 348–356, Sep. 2017, doi: 10.1016/j.isatra.2017.07.003.
- [23] V. Utkin, J. Guldner, and J. Shi, Sliding Mode Control in Electro-Mechanical Systems, 2nd ed. Boca Raton: CRC Press, 2017. doi: 10.1201/9781420065619.
- [24] P. Briš, J. Vittek, and P. Makyš, "Position Control of PMSM in Sliding Mode", Adv. Electr. Electron. Eng., vol. 7, Jan. 2008.
- [25] A. Kolesnikov, G. Veselov, and A. Kolesnikov, "Modern applied control theory: synergetic approach in control theory", TRTU Mosc. Taganrog, pp. 4477–4479, 2000.
- [26] A. Hadjira, F. Khaber, M. Mustapha, K. Kassmi, and N. Essounbouli, "Development and experimentation of a new MPPT synergetic control for photovoltaic systems", J. Optoelectron. Adv. Mater., vol. 18, pp. 165–173, Jan. 2016.
- [27] E. Akoro, T. Gabriel Jean-Philippe, M. Faye, M. Doumbia, and S. M. Amadou, "Artificial Neural Network Photovoltaic Generator Maximum Power Point Tracking Method using Synergetic Control Algorithm", Jan. 2020.
- [28] M. S. Mahgoun and A. E. Badoud, "New design and comparative study via two techniques for wind energy conversion system", Electr. Eng. Electromechanics, no. 3, Art. no. 3, Jun. 2021, doi: 10.20998/2074-272X.2021.3.03.
- [29] M. M. Seddik and B. A. Essalam, "Synthesis and high-performance analysis of Synergetic control MPPT for PMSG-based Wind Energy Conversion Systems", in 2022 19th International Multi-Conference on Systems, Signals & Devices (SSD), May 2022, pp. 309–314. doi: 10.1109/SSD54932.2022.9955822.
- [30] M. Zhao and T. Wang, "A sliding mode and synergetic control approaches applied to Permanent Magnet Synchronous Motor", J. Phys. Conf. Ser., vol. 1087, p. 042012, Sep. 2018, doi: 10.1088/1742-6596/1087/4/042012.
- [31] T. Bogani, A. Lidozzi, L. Solero, and A. Di Napoli, "Synergetic Control of PMSM Drives for High Dynamic Applications", in IEEE International Conference on Electric Machines and Drives, 2005., May 2005, pp. 710–717. doi: 10.1109/IEMDC.2005.195801.
- [32] M. S. Perdigão, J. P. Trovão, J. M. Alonso, P. G. Pereirinha, and E. S. Saraiva, "Experimental large-signal characterization of power inductors in bidirectional electric vehicle DC-DC converters for simulation analysis", in 2013 15th European Conference on Power Electronics and Applications (EPE), Sep. 2013, pp. 1–10. doi: 10.1109/EPE.2013.6634438.
- [33] M. A. Silva, J. P. Trovão, and P. G. Pereirinha, "Implementation of a multiple input DC-DC converter for Electric Vehicle power system", in Proceedings of the 2011 3rd International Youth Conference on Energetics (IYCE), Jul. 2011, pp. 1–8. Accessed: Aug. 16, 2024. [Online]. Available: https://ieeexplore.ieee.org/document/6028283
- [34] I. Azizi and H. Radjeai, "A new strategy for battery and supercapacitor energy management for an urban electric vehicle", Electr. Eng., vol. 100, no. 2, pp. 667–676, Jun. 2018, doi: 10.1007/s00202-017-0535-1.
- [35] J. P. Trovao, P. G. Pereirinha, and F. J. T. E. Ferreira, "Comparative study of different electric machines in the powertrain of a small electric vehicle", in 2008 18th International Conference on Electrical Machines, Sep. 2008, pp. 1–6. doi: 10.1109/ICELMACH.2008.4800164.
- [36] R. Krishnan, Permanent Magnet Synchronous and Brushless DC Motor Drives. CRC Press, 2009.
- [37] V. Perelmuter, Electrotechnical Systems: Simulation with Simulink® and SimPowerSystemsTM. Boca Raton: CRC Press, 2020. doi: 10.1201/b13013.
- [38] M. S. Zaky, "Adaptive Switching Plane of Integral Variable Structure Control for Speed Control of Permanent Magnet Synchronous Motor Drives", Electr. Power Compon. Syst., vol. 39, no. 13, pp. 1353–1372, Aug. 2011, doi: 10.1080/15325008.2011.584107.

- [39] Y.-D. Son, T.-W. Heo, E. Santi, and A. Monti, "Synergetic control approach for induction motor speed control", in 30th Annual Conference of IEEE Industrial Electronics Society, 2004. IECON 2004, Nov. 2004, pp. 883-887 Vol. 1. doi: 10.1109/IECON.2004.1433432.
- [40] L. Medjbeur, H. Mohamed N., and S. Benaggoune, "Robust induction motor control using adaptive fuzzy synergetic control", J. Electr. Eng., vol. 12, pp. 37–42, Jan. 2012.
- [41] X. Yu, Z. Jiang, and Y. Zhang, "A synergetic control approach to grid-connected, wind-turbine doubly-fed induction generators", in 2008 IEEE Power Electronics Specialists Conference, Jun. 2008, pp. 2070–2076. doi: 10.1109/PESC.2008.4592248.
- [42] A. Nusawardhana, S. H. Zak, and W. Crossley, "Nonlinear Synergetic Optimal Controllers", J. Guid. Control Dyn., vol. 30, pp. 1134–1147, Jul. 2007, doi: 10.2514/1.27829.
- [43] A. Davoudi, A. M. Bazzi, and P. L. Chapman, "Application of synergetic control theory to non-sinusoidal PMSMs via multiple reference frame theory", in 2008 34th Annual Conference of IEEE Industrial Electronics, Nov. 2008, pp. 2794–2799. doi: 10.1109/IECON.2008.4758401.
- [44] B. Farid and E. Merabet, "Design of a New Direct Torque Control Using Synergetic Theory for Double Star Induction Motor", J. Eur. Systèmes Autom., vol. 53, pp. 903–914, Dec. 2020, doi: 10.18280/jesa.530616.
- [45] J. Larminie and J. Lowry, Electric vehicle technology explained, Second edition. Chichester, West Sussex, United Kingdom: Wiley, a John Wiley & Sons, Ltd., Publication, 2012.
- [46] A. Haddoun, M. E. H. Benbouzid, D. Diallo, R. Abdessemed, J. Ghouili, and K. Srairi, "A Loss-Minimization DTC Scheme for EV Induction Motors", IEEE Trans. Veh. Technol., vol. 56, no. 1, pp. 81–88, Jan. 2007, doi: 10.1109/TVT.2006.889562.
- [47] I. Azizi and H. Radjeai, "A bidirectional DC-DC converter fed DC motor for electric vehicle application", in 2015 4th International Conference on Electrical Engineering (ICEE), Dec. 2015, pp. 1–5. doi: 10.1109/INTEE.2015.7416683.
- [48] P. Fajri, R. Ahmadi, and M. Ferdowsi, "Equivalent vehicle rotational inertia used for electric vehicle test bench dynamic studies", in IECON 2012 38th Annual Conference on IEEE Industrial Electronics Society, Oct. 2012, pp. 4115–4120. doi: 10.1109/IECON.2012.6389231.